Magna Scientia Advanced Research and Reviews

eISSN: 2582-9394

Cross Ref DOI: 10.30574/msarr

Journal homepage: https://magnascientiapub.com/journals/msarr/

(REVIEW ARTICLE)

Check for updates

Modeling and applications of Electrochemical Impedance Spectroscopy (EIS) for Zinc-ion batteries

Mahnaz Zameni *

Department of Computer Science, College of Engineering, Azad University of Sari, Iran.

Magna Scientia Advanced Research and Reviews, 2024, 10(01), 123–131

Publication history: Received on 14 December 2023; revised on 27 January 2024; accepted on 30 January 2024

Article DOI: https://doi.org/10.30574/msarr.2024.10.1.0017

Abstract

Electrochemical Impedance Spectroscopy (EIS) has emerged as a valuable tool for evaluating secondary batteries due to their efficiency and accuracy. However, interpreting the multifaceted impedance spectra derived from EIS demands a comprehensive grasp of the electrochemical context. This study focuses on devising and applying an Electrochemical Impedance Spectroscopy (EIS) model customized specifically for deciphering the intricacies of zinc-ion batteries. The model construction is tailored to the battery's complexities, enabling extraction of circuit elements that faithfully depict the system's dynamics. Moreover, this research investigates the relationship between parameters of the governing equations. Through experimental validation employing real-time EIS measurements from a zinc-ion battery prototype, the reliability and efficacy of the proposed model are confirmed. This validated model not only enhances our understanding of zinc-ion battery behavior but also propels advancements in utilizing this technology across various energy storage applications.

Keywords: Electrochemical Impedance Spectroscopy; Zinc Ion Battery; Behavior Modeling; Charge Transfer Kinetics; Equivalent Circuit Model; Diffusion Coefficient

1. Introduction

The deregulation of the electric market and the push towards a de-carbonized electric power system have introduced significant challenges in energy conversion and storage systems [1-8]. Integrating renewable energies into the grid can play a significant role in resolving these challenges [9-12]. As the goal is to achieve a fully renewable energy supply by 2050 [13], effective storage solutions are critical for maintaining reliability amidst renewable expansion, forming the backbone of a resilient energy infrastructure [14-16]. In the landscape of large-scale energy storage solutions, the significance of zinc-ion batteries has surged, heralding a promising era marked by their potential for high energy density and cost-effectiveness [17, 18]. Utilizing these batteries in grid-scale applications necessitates a meticulous understanding of their behavior and performance [19, 20]. One of the foremost characterization techniques vital in comprehending and optimizing zinc-ion batteries is Electrochemical Impedance Spectroscopy (EIS). This technique plays a pivotal role in unraveling the intricacies of battery dynamics, guiding advancements crucial for their effective integration into large-scale energy storage systems [21-23].

Impedance spectroscopy is not limited to battery analysis; its significance extends to material characterization and the study of various electrochemical cells like fuel cells, offering crucial insights into their performance and behavior [24, 25]. At the heart of zinc-ion battery behavior lies the movement of ions within the electrolyte and electrode materials. Governing equations encapsulating these ion movements elucidate the fundamental dynamics of these batteries [26-28]. The diffusion of zinc ions across the electrolyte and their intercalation into electrode materials are meticulously governed by mass transport equations [29-32]. Understanding and modeling these ion movement equations are

* Corresponding author: Zameni Mahnaz

instrumental in comprehending the intricate transport phenomena dictating the performance and lifespan of zinc-ion batteries.

The interpretation of zinc-ion battery behavior using Electrochemical Impedance Spectroscopy (EIS) emerges as a cornerstone in identifying crucial performance indicators [33-36]. EIS not only enables the quantification of key parameters but also serves as a diagnostic tool, shedding light on impedance changes, resistance buildup, ion movement constraints, and capacity fade over cycling [37-39]. The elucidation of these phenomena through EIS facilitates the identification of underlying causes, such as electrode degradation, electrolyte interface evolution, and other factors contributing to impedance growth and performance degradation [25, 40, 41].

Understanding these facets is pivotal for optimizing zinc-ion battery design and operation, addressing challenges associated with resistance increase and ion movement constraints. EIS emerges as an indispensable tool, offering insights essential for advancing the performance and reliability of zinc-ion batteries in large-scale energy storage applications [29, 42, 43].

Within the domain of zinc-ion batteries, a notable gap persists in the comprehensive understanding and simulation of fundamental electrochemical processes . This paper endeavors to bridge this gap by delving into the modeling intricacies encapsulated within the governing equations governing ion movement, charge transfer kinetics, and impedance phenomena. By integrating these critical equations into a comprehensive framework and subsequently validating the model against experimental data, this study aims to contribute significantly to the foundational comprehension of zinc-ion battery behavior. Additionally, the research endeavors to elucidate the paramount significance of various parameters governing battery performance, shedding light on their interplay and impact on overall battery characteristics. The endeavor to unravel and comprehend these nuances not only advances the fundamental understanding of zinc-ion batteries but also lays the groundwork for future innovations and optimizations essential for their widespread integration into energy storage applications.

2. Principal of EIS

In essence, a Zinc-ion battery comprises vital components: a cathode, an anode, a separator, current collectors, and an electrolyte. As the battery undergoes electrochemical reactions, both electrons and Zinc ions traverse these components, each possessing resistive and capacitive characteristics [44]. Essentially, the elements within the battery, alongside the double layer present at the interface, form the essential circuit elements constituting the Zinc-ion battery's circuit model. These elements are interconnected in parallel and/or series configurations. While the impedance attributes of these circuit elements differ based on cell types and component characteristics, an overall impedance value can be derived by scanning the AC frequency within the 100 kHz to 10 mHz range [29]. The range for Electrochemical Impedance Spectroscopy (EIS) analysis is reliant on the typical response time dictated by the cell's constituents. Consequently, the low-frequency range, spanning from 10 Hz to 10 mHz, corresponds to the slower chemical zinc diffusion denoted as Warburg impedance. Subsequently, impedance related to charge transfer reactions emerges in the mid-frequency range, around 10 kHz to 10 Hz, followed by the relatively rapid transport process through the interface layer, measured at high frequencies of 100 kHz to 10 kHz. Analyzing impedance values within these frequency ranges entails employing EIS spectral fitting methodologies based on an established equivalent circuit model [45].

Electrochemical Impedance Spectroscopy (EIS) is a method used to measure resistance (R), capacitance (C), and inductance (L) by observing how a cell responds to an applied AC voltage. When a DC voltage is applied, Ohm's law governs the relationship between resistance (R), voltage (V), and current (I), as seen in conventional circuits. Similarly, in an AC-driven electrochemical cell, impedance $Z(\omega)$ (where $\omega = 2\pi f$ represents the angular frequency of the AC voltage) is expressed as $V(\omega) / I(\omega)$, reflecting the principles of Ohm's law adapted for an AC circuit. Impedance represents the resistance that impedes current flow when an AC voltage is applied, characterized by various circuit elements—such as resistors, inductors, and conductors—forming the overall impedance in the circuit. Real electrochemical systems comprise a combination of diverse circuit elements, making the use of impedance a more accurate representation than solely relying on a resistor in a circuit model. Additionally, when V is applied at angular frequency ω, V and I exhibit a phase difference Ø, denoting a specific relationship between them. Here, Vm and Im represent the maximum values of V and I, respectively.

The impedance spectrum can be illustrated in two distinct formats: firstly, the "Bode plot," displaying alterations in phase shift and magnitude across various applied frequency ranges, and secondly, the "Nyquist plot," graphing the real and imaginary components of $Z(\omega)$ using Cartesian coordinates. The Bode plot offers significant advantages in observing phase margins, especially when the system shows signs of instability through abrupt phase or magnitude changes. This characteristic makes it particularly valuable for scrutinizing sensors, filters, and transistors within

electronic devices. On the other hand, the Nyquist plot offers deeper insights into potential mechanisms or governing phenomena within an equivalent circuit model system. In the context of analyzing zinc-ion batteries, the Nyquist plot is more commonly employed due to its convenience in examining active reaction mechanisms, providing a clearer understanding of their characteristics [46].

Under specific scenarios where semi-infinite linear diffusion influences an electrochemical system, affecting both kinetic and diffusion control mechanisms, the Warburg impedance finds its place within the equivalent circuit model [47]. Figure 1 shows the circuit model and the Bode plot and Nyquist plot for this cell. To represent the mass transfer resistance due to diffusion limitation, the Warburg impedance takes on a distinct appearance a linear representation inclined at a 45-degree angle. Beyond simply accommodating bulk and polarization resistance losses, this model accommodates the polarization inherent in the zinc diffusion reaction.

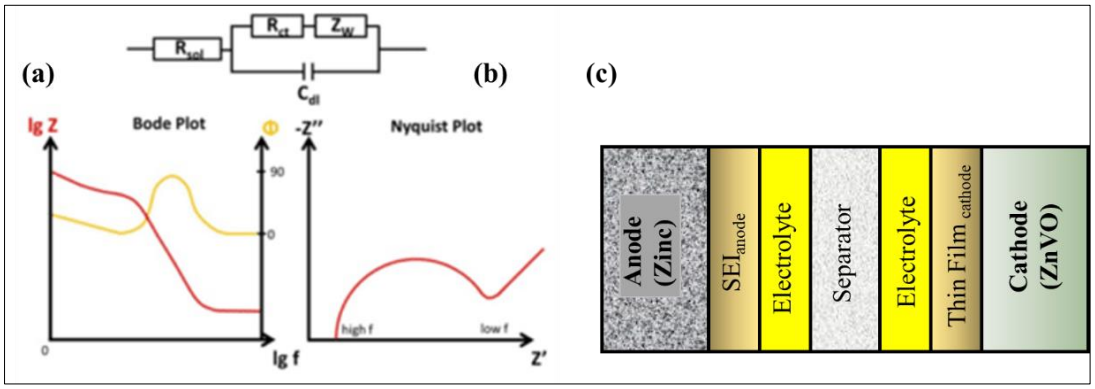

Figure 1 a)Bode plot and b) Nyquist plot of a full cell battery and equivalent circuit (33) c) schematic of a zinc ion battery

3. Characterization of the Resistances

The semicircle of the EIS spectrum is caused by the impedance of a layer that forms on the interface between the electrode and electrolyte. The first resistance depicted in Figure 1 is the ohmic resistance, which is a representation of ionic movement resistance. The breakdown of the electrolyte produces this layer, which is known as the solid electrolyte interface (SEI) layer. The SEI layer affects the electrochemical characteristics of the anode material more than the cathode does. The surface coating, gradient, surface area, and other characteristics of the layer are changed. Additionally, some nanostructured anode materials, such as Fe_2O_3, MnO, and Co_3O_4, show reversible film formation, adding additional capacity above and beyond the theoretical capacity [48]. To study the behavior of the cell a constant potential is applied with changes in frequency. At low frequencies (10 Hz to 10 mHz), the response primarily reflects slow chemical processes like diffusion, often represented as the Warburg impedance. The diffusion of ions or molecules through the electrolyte or interfaces dominates the cell's behavior in this frequency range. This range represents slow transport phenomena, particularly the gradual movement of ions, typically observed through a linear trend in the impedance plot. In the mid-frequency range (10 Hz to 10 kHz), impedance reflects the charge transfer reactions occurring at interfaces or electrode surfaces. This range encompasses the kinetics of electrochemical reactions, such as the conversion between chemical species at the electrode-electrolyte interface. Analysis within this range provides insights into the reaction kinetics, with impedance behavior indicating the efficiency and speed of charge transfer processes. At higher frequencies, impedance is indicative of the relatively rapid transport processes through the interface layer. These frequencies often relate to the dynamics of the interface between the electrode and electrolyte, where quicker phenomena like adsorption/desorption occur. Analysis in this range sheds light on the efficiency of surface reactions and the behavior of species moving across the electrode-electrolyte boundary. Mass transfer equations at various frequencies enable the construction of equivalent circuit models that describe the cell's behavior. By applying voltage at different frequencies and analyzing the cell's response using mass transfer equations, researchers can gain insights into the underlying mechanisms governing ion transport, charge transfer, and electrochemical reactions within the electrochemical cell [49].

4. Results

4.1. Experimental Data

In this study, the experimental data utilized in the analysis of electrode degradation rates was obtained from the comprehensive work conducted by Rajabi et al. [29]. The experimental data detailed by Rajabi et al. involved impedance spectroscopy tests conducted for different electrolytes of a zinc ion battery.

4.2. Modeling Data

Our research employs a one-dimensional modeling approach implemented using COMSOL Multiphysics, utilizing a finite element numerical technique to simulate the impedance spectroscopy behavior in our electrochemical system. The governing equations utilized in our model encompass the general mass transfer equation to and diffusion equation governing the transport of ions through the electrolyte, represented by Fick's second law as depicted below:

$$\nabla . J_i + u . \nabla c_i = R_i$$

$$J_i = -D_i \nabla \emptyset_i \tag{1}$$

J is the diffusion flux (mole/m^2s) and D is the diffusion (m^2/s) coefficient of the species I and the last term is the concentration gradient and R is the amount of produced species i. This equation elucidates the concentration gradients of ions as a function of space and time within the electrolyte.

Additionally, the model incorporates the Butler-Volmer equation (shown below) to characterize the kinetics of charge transfer at the electrode-electrolyte interface. This equation embodies the electrochemical reactions occurring at the interface, accounting for the transfer of charges between the electrode and electrolyte species.

$$i_b = i_0 \left\{ \frac{c_0(0,t)}{c_0^*} \exp\left[\frac{\alpha_a z F E}{RT}\right] - \frac{c_r(0,t)}{c_r^*} \exp\left[\frac{\alpha_r z F E}{RT}\right] \right\} \tag{3}$$

i is the current density A/m^2, c_0 and c_r refer to the concentration of the species to be oxidized and reduced, $c_0(0,t)$ is the time dependent concentration at the distance zero from the surface, E is over potential, and F is faraday constant.

Capacitance is observed in an impedance spectroscopy of a full cell battery as a result of charge accumulation at the interface, multiple battery interfaces, and diffusion layers.

$$i_{dl} = i\omega(\varphi_s - \varphi_I) C_{dl} \tag{4}$$

$$i_{total} = i_{dl} + i_b \tag{5}$$

The total current is the sum of capacitance current and current originated from voltage difference between the electrode, the bulk electrolyte and capacitance current.

In this work, the data was obtained from an experimental test result, however double layer capacitance was optimized by comparing the numerical results with experimental data. The data is summarized in table 1.

Table 1 Model input data

Name	Amount	Units	Description
D	1e-10	m2/s	Diffusion Coefficient
Cbulk	2	mole/ m3	Bulk Concentration
Cdl	0.025	F/m2	Double layer interfacial capacitance
K0	0.00001	m/s	Heterogeneous rate of reaction
i_0	4.19	mA/cm2	Exchange current density
Fmin	1	Hz	Minimum frequency
Fmax	100000	Hz	Maximum frequency
Xdiffmax	Sqrt(D/(2*pi*log (Fmin)))	m	Maximum thickness of diffusion layer
Xdiffmin	Sqrt(D/(2*pi*log(Fmax)))	m	Minimum thickness of diffusion layer
Lel	2*Xdiffmax	m	Domain length
Ael	0.000531	m2	Electrode surface area
Vapp	0.005	V	Applied voltage

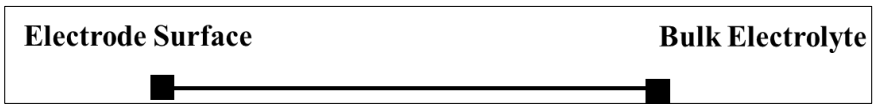

Figure 2 Schematic illustration of the model with the boundary condition

This 1D model demonstrated in Figure 2, was meshed extremely fine with even finer mesh around the electrode. And constant concentration was defined for the right side of the domain. As shown in Figure 3a, the responses generated by our model closely matched the actual responses obtained from experiments. This close correspondence affirms the model's efficacy to study further on the important parameters. The depth of the diffusion layer, and Bode plot are shown in Figure 3b, and 3c with considering the same condition of the real battery of zinc ion battery and with 2M zinc sulfate as electrolyte and glass fiber as separator. Figure 3b illustrates the concentration of the oxidation and reduction species (Zn^{2+} and Zn) vs the distance from the electrode.

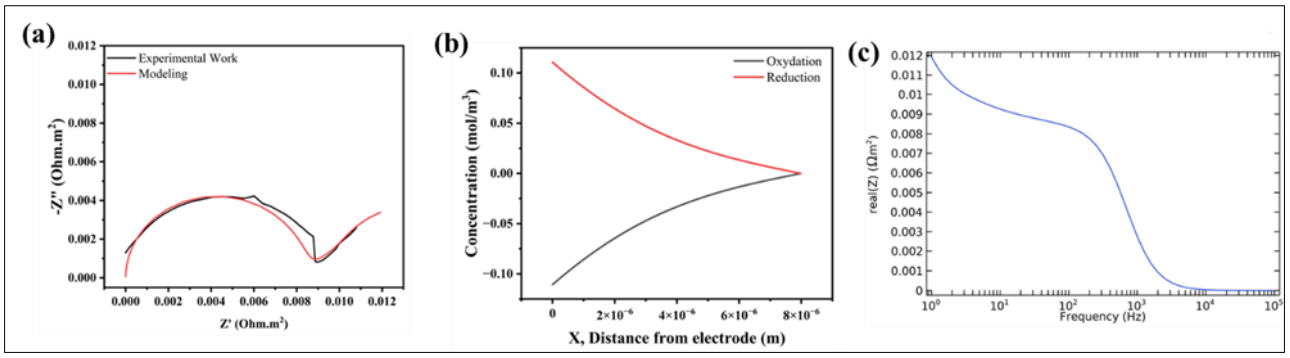

Figure 3 a) Nyquist Plot, verification of the model with experimental data b) the concentration of redux and oxidation species vs distance from the electrode surface c) Bode plot

In this study, our focus was on evaluating the impact of key parameters on battery performance, aiming to understand their influence without directly altering the battery's constituent materials. The first parameter to study is the heterogeneous rate constant, which represents the kinetics of charge transfer at the electrode- electrolyte interface, playing a significant role in the impedance spectroscopy of a full battery. A higher heterogeneous rate constant typically leads to a lower charge transfer resistance (R_ct) at the electrode interface. Consequently, a decrease in R_ct is observed

in the impedance spectra as depicted in Figure 4a. The relationship between the rate constant and confirms these results as well as shown below:

$$R_{ct} = \frac{RT}{n^2F^2ACk^0} \tag{6}$$

Mathematically, it is totally clear that increasing the rate constant would lead to a lower charge transfer resistance [50, 51, 52], to explain more electrochemically, the higher rate constants facilitate faster charge transfer kinetics, reducing the resistance to the transfer of charges across the electrode-electrolyte interface. This manifests as a distinct decrease in the impedance spectra, especially in the mid-frequency range associated with charge transfer reactions. variations in the rate constant may lead to shifts in the capacitance features within the impedance spectra, particularly affecting the high-frequency regions associated with the double-layer capacitance. The second important parameter is the change of electrolyte concentration. Changes in bulk concentration affect the total amount of ions available for electrochemical reactions, which has subtle effects on impedance spectra in various frequency ranges. Increased bulk concentrations usually result in an increase in the total impedance magnitude, especially in the low-frequency regions, indicating modifications to the diffusion processes and electrolyte accessibility. Higher electrolyte concentrations often lead to increased ionic conductivity within the cell. This results in reduced overall impedance across the frequency spectrum, particularly at lower frequencies associated with ionic movement and transport as depicted in Figure 4b. However, it should be considered that higher concentration after a specific point would lead to a higher viscosity that would decrease the diffusivity. Furthermore, changes in the diffusion coefficient affect ion mobility. The Warburg impedance, typically observed at lower frequencies, represents diffusional limitations or ion transport through electrolyte. Changes in the diffusion coefficient directly impact the Warburg impedance. Higher diffusion coefficients facilitate increased ion mobility, leading to a reduction in the Warburg impedance, indicating improved diffusional kinetics as can be seen in Figure 4c. Understanding these effects is crucial for evaluating ion transport dynamics, assessing diffusion limitations, and comprehending the electrochemical behavior of the system under study.

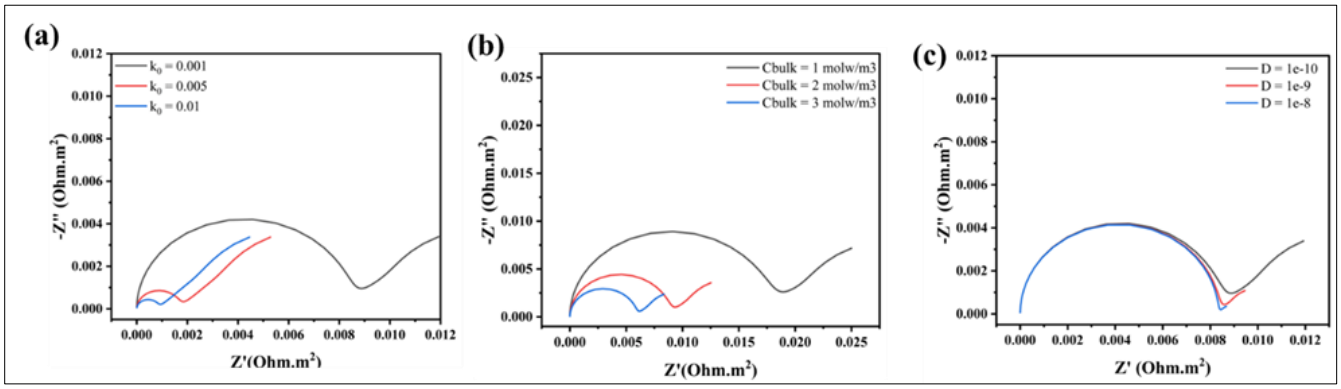

Figure 4 The effect of different parameters a) The effect of rate of reaction, b) The effect of bulk concentration, c) The effect of diffusion coefficient

5. Conclusion

When evaluating secondary batteries, Electrochemical Impedance Spectroscopy (EIS) is a highly accurate and potent tool that provides deep insights into battery efficiency. But deciphering the complex impedance spectra obtained from EIS requires a thorough comprehension of the electrochemical background. This work explores the development and application of an Electrochemical Impedance Spectroscopy (EIS) model that is finely tuned to unravel the mysteries of zinc-ion batteries. Through circuit element extraction, the built model, tailored to the battery's complexities, faithfully captures the dynamics of the system. Our results validate the effectiveness and reliability of the proposed model experimentally using real-time EIS measurements from a prototype zinc-ion battery. This verified model not only helps us better understand how zinc-ion batteries behave, but it also speeds up the adoption of this technology for a variety of energy storage applications.

Compliance with ethical standards

Disclosure of conflict of interest

No conflict of interest to be disclosed.

References

[1] Yang G, El Loubani M, Chalaki HR, Kim J, Keum JK, Rouleau CM, et al. Tuning Ionic Conductivity in Fluorite Gd-Doped CeO2-Bixbyite RE2O3 (RE= Y and Sm) Multilayer Thin Films by Controlling Interfacial Strain. ACS Applied Electronic Materials. 2023;5(8):4556-63.

[2] Babazadeh Dizaj R. DEVELOPMENT OF LSF-BASED DUAL-PHASE CATHODES FOR INTERMEDIATE TEMPERATURE SOLID OXIDE FUEL CELLS: Middle East Technical University; 2022.

[3] Dizaj RB, Sabahi N. Optimizing LSM-LSF composite cathodes for enhanced solid oxide fuel cell performance: Material engineering and electrochemical insights. 2023.

[4] Seyed Mostafa Nasrollahpour Shirvani MG, Hamed Afrasiab, Ramazanali Jafari Talookolaei. Optimization of a Composite Sandwich Panel with Honeycomb Core Under Out-of-Plane Pressure with NMPSO Algorithm. The 28th Annual International Conference of Iranian Society of Mechanical Engineers (ISME)2020.

[5] Shirvani SMN, Gholami M, Afrasiab H, Talookolaei RAJ. Optimal design of a composite sandwich panel with a hexagonal honeycomb core for aerospace applications. Iranian Journal of Science and Technology, Transactions of Mechanical Engineering. 2023;47(2):557-68.

[6] Shirvani SMN, Nakhi A, Karimi A, Mobli M. Optimizing methane direct utilization: The advanced Sr2CoMoO6-δ anode. 2023.

[7] Nakhi A, Mostafa S, Karimi A, Mobli M. Unveiling the Promoted LSTM/YSZ Composite Anode for Direct Utilization of Hydrocarbon Fuels. International Journal of Science and Engineering Applications. 2023;12(12):18 - 24.

[8] Nazari B, Abdolalian S, Taghavijeloudar M. An environmentally friendly approach for industrial wastewater treatment and bio-adsorption of heavy metals using Pistacia soft shell (PSS) through flocculation-adsorption process. Environmental Research. 2023;235:116595.

[9] Geri A, Gatta FM, Maccioni M, Dell'Olmo J, Carere F, Bucarelli MA, et al., editors. Distributed generation monitoring: a cost-effective Raspberry Pi-based device. 2022 2nd International Conference on Innovative Research in Applied Science, Engineering and Technology (IRASET); 2022: IEEE.

[10] Taghavi H. Liquid Cooling System for a High Power, Medium Frequency, and Medium Voltage Isolated Power Converter [M.S.]. United States -- South Carolina: University of South Carolina; 2023.

[11] Taghavi H, El Shafei A, Nasiri A, editors. Liquid Cooling System for a High Power, Medium Frequency, and Medium Voltage Isolated Power Converter. 2023 12th International Conference on Renewable Energy Research and Applications (ICRERA); 2023: IEEE.

[12] Bhuvela P, Taghavi H, Nasiri A, editors. Design Methodology for a Medium Voltage Single Stage LLC Resonant Solar PV Inverter. 2023 12th International Conference on Renewable Energy Research and Applications (ICRERA); 2023: IEEE.

[13] Rajabi R, Thompson J, Krarti M. Benefit Cost Analysis of Electrification of Urban Districts: Case Study of Philadelphia, Pennsylvania. Journal of Engineering for Sustainable Buildings and Cities. 2020;1(4):041004.

[14] Taghavi M, Gharehghani A, Nejad FB, Mirsalim M. Developing a model to predict the start of combustion in HCCI engine using ANN-GA approach. Energy Conversion and Management. 2019;195:57-69.

[15] Taghavi M, Perera LP, editors. Data Driven Digital Twin Applications Towards Green Ship Operations. International Conference on Offshore Mechanics and Arctic Engineering; 2022: American Society of Mechanical Engineers.

[16] Taghavi M, Perera LP, editors. Multiple Model Adaptive Estimation Coupled With Nonlinear Function Approximation and Gaussian Mixture Models for Predicting Fuel Consumption in Marine Engines. International Conference on Offshore Mechanics and Arctic Engineering; 2023: American Society of Mechanical Engineers.

[17] Huang S, Hou L, Li T, Jiao Y, Wu P. Antifreezing hydrogel electrolyte with ternary hydrogen bonding for high-performance zinc-ion batteries. Advanced Materials. 2022;34(14):2110140.

[18] Salmasi F, Sabahi N, Abraham J. Discharge coefficients for rectangular broad-crested gabion weirs: experimental study. Journal of Irrigation and Drainage Engineering. 2021;147(3):04021001.

[19] Xu L, Meng T, Zheng X, Li T, Brozena AH, Mao Y, et al. Nanocellulose-Carboxymethylcellulose Electrolyte for Stable, High-Rate Zinc-Ion Batteries. Advanced Functional Materials. 2023:2302098.

[20] Alvandifar N, Saffar-Avval M, Amani E, Mehdizadeh A, Ebrahimipour M, Entezari S, et al. Experimental study of partially metal foam wrapped tube bundles. International Journal of Thermal Sciences. 2021;162:106798.

[21] Chang B-Y, Park S-M. Electrochemical impedance spectroscopy. Annual Review of Analytical Chemistry. 2010;3:207-29.

[22] Wang S, Zhang J, Gharbi O, Vivier V, Gao M, Orazem ME. Electrochemical impedance spectroscopy. Nature Reviews Methods Primers. 2021;1(1):41.

[23] Orazem ME, Tribollet B. Electrochemical impedance spectroscopy. New Jersey. 2008;1:383-9.

[24] Chalaki HR, Babaei A, Ataie A, Seyed-Vakili S-V, editors. The Effect of Impregnation of Ceramic Nano-particles on the Performance of LSCM/YSZ Anode Electrode of Solid Oxide Fuel Cell. 5th International Conference on Materials Engineering and Metallurgy; 2016.

[25] Rostaghi Chalaki H, Babaei A, Ataie A, Seyed-Vakili SV. LaFe 0.6 Co 0.4 O 3 promoted LSCM/YSZ anode for direct utilization of methanol in solid oxide fuel cells. Ionics. 2020;26:1011-8.

[26] Aminnia N. CFD-XDEM coupling approach towards melt pool simulations of selective laser melting. 2023.

[27] Aminnia N, Adhav P, Darlik F, Mashhood M, Saraei SH, Besseron X, et al. Three-dimensional CFD-DEM simulation of raceway transport phenomena in a blast furnace. Fuel. 2023;334:126574.

[28] Aminnia N, Estupinan Donoso AA, Peters B. Developing a DEM-Coupled OpenFOAM solver for multiphysics simulation of additive manufacturing process. Scipedia com. 2022.

[29] Rajabi R, Sun S, Billings A, Mattick VF, Khan J, Huang K. Insights into Chemical and Electrochemical Interactions between Zn Anode and Electrolytes in Aqueous Zn− ion Batteries. Journal of The Electrochemical Society. 2022;169(11):110536.

[30] Aminnia N, Estupinan Donoso AA, Peters B. CFD-DEM simulation of melt pool formation and evolution in powder bed fusion process. 2022.

[31] Aminnia N, Peters B, ESTUPINAN AA. Multi-Scale Modeling of Melt Pool Formation and Solidification in Powder Bed Fusion: A Fully Coupled Computational Fluid Dynamics-Extended Discrete Element Method Approach. Available at SSRN 4502227.

[32] Aminnia N, Shateri M, Gheibi S, Torabi F. Modeling of Two-Phase flow in the Cathode Gas Diffusion Layer to Investigate Its Effects on a PEM Fuel Cell.

[33] Ciucci F. Modeling electrochemical impedance spectroscopy. Current Opinion in Electrochemistry. 2019;13:132-9.

[34] Estupinan Donoso AA, Aminnia N, Peters B, Michels A. On the Reduction of Computational Costs for Tungsten Powder Bed Processes. 2022.

[35] Mahamud R, Mobli M, Farouk TI, editors. Modes of oscillation in a high pressure microplasma discharges. 2014 IEEE 41st International Conference on Plasma Sciences (ICOPS) held with 2014 IEEE International Conference on High-Power Particle Beams (BEAMS); 2014: IEEE.

[36] Mobli M. Thermal analysis of high pressure micro plasma discharge. 2014.

[37] Mobli M. Characterization Of Evaporation/Condensation During Pool Boiling And Flow Boiling: University of South Carolina; 2018.

[38] Mobli M, Bayat M, Li C. Estimating bubble interfacial heat transfer coefficient in pool boiling. Journal of Molecular Liquids. 2022;350:118541.

[39] Mobli M, Farouk T, editors. High pressure micro glow discharge: Detailed approach to gas temperature modeling. APS Annual Gaseous Electronics Meeting Abstracts; 2014.

[40] Mobli M, Li C, editors. On the heat transfer characteristics of a single bubble growth and departure during pool boiling. International Conference on Nanochannels, Microchannels, and Minichannels; 2016: American Society of Mechanical Engineers.

[41] Mobli M, Mahamud R, Farouk T, editors. High pressure micro plasma discharge: Effect of conjugate heat transfer. 2013 19th IEEE Pulsed Power Conference (PPC); 2013: IEEE.

[42] Namazi H, Perera LP, editors. Trustworthiness Evaluation Framework for Digital Ship Navigators in Bridge Simulator Environments. International Conference on Offshore Mechanics and Arctic Engineering; 2023: American Society of Mechanical Engineers.

[43] Namazi H, Taghavipour A. Traffic flow and emissions improvement via vehicle-to-vehicle and vehicle-to-infrastructure communication for an intelligent intersection. Asian Journal of Control. 2021;23(5):2328-42.

[44] Wang F, Zhang J, Lu H, Zhu H, Chen Z, Wang L, et al. Production of gas-releasing electrolyte-replenishing Ah-scale zinc metal pouch cells with aqueous gel electrolyte. Nature Communications. 2023;14(1):4211.

[45] Macdonald DD. Reflections on the history of electrochemical impedance spectroscopy. Electrochimica Acta. 2006;51(8-9):1376-88.

[46] Tian J, Lv L, Fei C, Wang Y, Liu X, Cao G. A highly efficient (> 6%) Cd 1− x Mn x Se quantum dot sensitized solar cell. Journal of Materials Chemistry A. 2014;2(46):19653-9.

[47] Choi W, Shin H-C, Kim JM, Choi J-Y, Yoon W-S. Modeling and applications of electrochemical impedance spectroscopy (EIS) for lithium-ion batteries. Journal of Electrochemical Science and Technology. 2020;11(1):1-13.

[48] Hou C, Wang B, Murugadoss V, Vupputuri S, Chao Y, Guo Z, et al. Recent advances in Co3O4 as anode materials for high-performance lithium-ion batteries. Engineered Science. 2020;11(5):19-30.

[49] Hernández HH, Reynoso AR, González JT, Morán CG, Hernández JM, Ruiz AM, et al. Electrochemical impedance spectroscopy (EIS): A review study of basic aspects of the corrosion mechanism applied to steels. Electrochemical Impedance Spectroscopy. 2020:137-44.

[50] Randviir EP. A cross examination of electron transfer rate constants for carbon screen-printed electrodes using Electrochemical Impedance Spectroscopy and cyclic voltammetry. Electrochimica Acta. 2018;286:179-86.

[51] Dizaj RB, Sabahi N. Laboratory preparation of LSM and LSF sputtering targets using PTFE rings for deposition of SOFC thin film electrodes. 2023.

[52] Nakhi A, Ganjali M, Shirinzadeh H, Sedaghat Ahangari Hossein Zadeh A, Mozafari M. Laser Cladding of Fluorapatite Nanopowders on Ti6Al4V. Advanced Materials Letters. 2020 Jan 1;11(1):1-5